Precision of subnational forest AGB estimates within the Peruvian Amazonia using a global biomass map

Natalia Málaga [a,*], Sytze de Bruin [a], Ronald E. McRoberts [b,c], Alexs Arana Olivos [d], Ricardo de la Cruz Paiva [d], Patricia Durán Montesinos [d], Daniela Requena Suarez [a], Martin Herold [a,e]

[a] *Laboratory of Geo-Information Science and Remote Sensing, Wageningen University and Research, Droevendaalsesteeg 3, 6708 PB Wageningen, the Netherlands*
[b] *Raspberry Ridge Analytics, Hugo, MN 55038, USA*
[c] *Department of Forest Resources, University of Minnesota, Saint Paul, MN 55108, USA*
[d] *Servicio Nacional Forestal y de Fauna Silvestre, Ministerio de Desarrollo Agrario y Riego (SERFOR), Lima, Peru*
[e] *Helmholtz Center Potsdam GFZ German Research Centre for Geosciences, Section 1.4 Remote Sensing and Geoinformatics, Telegrafenberg, Potsdam 14473, Germany*

ABSTRACT

National forest inventories (NFI) provide essential forest-related biomass and carbon information for country greenhouse gas (GHG) accounting systems. Several tropical countries struggle to execute their NFIs while the extent to which space-based global information on aboveground biomass (AGB) can support national GHG accounting is under investigation. We assess whether the use of a global AGB map as auxiliary information produces a gain in precision of subnational AGB estimates for the Peruvian Amazonia. We used model-assisted estimators with data from the country's NFI and explored hybrid inferential techniques to account for the sources of uncertainty associated with the integration of remote sensing-based products and NFI plot data.

Our results show that the selected global biomass map tends to overestimate AGB values across the Peruvian Amazonia. For most strata, directly using the map in its published form did not reduce the precision of AGB estimates. However, after calibrating the map using the NFI data, the precision of our map-assisted AGB estimates increased by up to 50% at stratum level and 20% at Amazonia level. We further demonstrate how different sources of uncertainties can be incorporated in the map-NFI integrated estimates. With the hybrid inferential analysis, we found that the small spatial support of the NFI plots compared to the remote sensing-based sample units of aggregated pixels (within block variability) contributed the most to the total uncertainty associated with the AGB estimates from our map-NFI integration. Uncertainties caused by measurement variability and allometric model prediction uncertainty were the second largest contributors. When these uncertainties were incorporated, the increase in precision of our calibrated map-assisted AGB estimates was negligible, probably hindered by the great contribution of the within block variability to our map-plot assessment. We developed a reproducible method that countries can build upon and further improve while the global biomass products continue to evolve and better characterize the AGB distribution under large biomass conditions. We encourage further cross-country case studies that reflect a wider range of AGB distributions, especially within humid tropical forests, to further assess the contribution of global biomass maps to (sub)national AGB estimates and finally GHG monitoring and reporting.

1. Introduction

Tropical countries have substantially increased the use of remote sensing information for forest monitoring while they develop national forest inventories (NFIs) to produce country specific greenhouse gas (GHG) estimates (Nesha et al., 2021; Romijn et al., 2015; Eggleston et al., 2006). The long-term success of forest-related monitoring systems depends on country efforts to upgrade or maintain their land use/forest area data and consistently update their NFIs (Romijn et al., 2015). Owing to budget constraints, inaccessibility of areas, institutional circumstances, developing capacities and the like, tropical countries struggle to establish national inventories or to guarantee frequent updates of their NFIs (Nesha et al., 2021; Ploton et al., 2020; Rodríguez-Veiga et al., 2017). These conditions limit the quality of their national

aboveground biomass (AGB) estimates, which ultimately hinders the accuracy, completeness and consistency of reported country GHG emissions and removals estimates under the international climate frameworks as well as the formulation of domestic mitigation targets.

Multiple efforts have been made to produce large-area biomass maps. As space-based biomass monitoring opportunities evolve, so does the policy framework with regard to the possible applications of remote sensing products for GHG monitoring and accounting (Herold et al., 2019). The refined 2019 Intergovernmental Panel on Climate Change (IPCC) guidelines propose the use of biomass maps for national land use, land use change and forestry (LULUCF) GHG reporting. Country case studies that link NFI plot-based data and satellite data are certainly needed to gain experience and build confidence on how national GHG monitoring and reporting can benefit from this fast-evolving research field. Given the limited coverage and periodicity of NFIs in tropical countries, it is timely to explore whether global biomass maps can improve sample-based inventory estimates. We assess how a large-area biomass map can be used as auxiliary data for the National Forest and Wildlife Inventory (NF&WI) in Peru as a means of increasing the precision of subnational AGB estimates. Previous studies have addressed the benefits of space-based data for increasing the precision of ground-based estimates (McRoberts et al., 2002; Ståhl et al., 2016; Næsset et al., 2016), but to our knowledge none of them are oriented to NFI applications in humid tropical forests, where forest ecosystems with the greatest AGB levels are mostly found.

The IPCC states that countries should reduce the uncertainties of their GHG inventories as far as practicable (Eggleston et al., 2006, Vol 1, Chap 1, Section 1.2). For uncertainties to be compared or reduced, they first must be rigorously estimated (McRoberts et al., 2018). Previous studies have addressed the use of hybrid inference when incorporating the uncertainty of allometric model predictions into the total uncertainty estimation (McRoberts et al., 2016; Ståhl et al., 2014), arguing that by ignoring this source of uncertainty, total uncertainty may be underestimated. We used hybrid inference to account for different sources of uncertainties from the integration of remote sensing-based products with ground-based data aiming for more comprehensive map-assisted estimates.

Peru started implementing the NF&WI in 2013, and by 2020 it had completed approximately 32% of the target sample. Though incomplete, the country relies on this probabilistic sample for estimating national forest-related emission factors (MINAM and MIDAGRI, 2021). Peru could benefit from the use of remote sensing-based biomass products to increase the precision of national and subnational AGB estimates, especially if they produce a more efficient (i.e., less intensive) sampling strategy. At the same time, in the latest update of the forest reference emission level, the country also recognized the need to more comprehensively account for and propagate the sources of uncertainties within its LULUCF-GHG accountability system (MINAM and MIDAGRI, 2021). Thus, an assessment of the effects of the sources of uncertainty from the integration of plot and space-based biomass data is key.

The objective of this study is to assess whether a large-area biomass map used as auxiliary data can produce a gain in precision relative to the precision of subnational field-based forest AGB estimates. To this end, we: i) defined a statistical inferential approach for the use of remotely sensed auxiliary information in combination with the NF&WI sample data; ii) locally calibrated an open-source, large-area biomass map using the NF&WI plot data; iii) accounted for the effects of the sources of uncertainty from the integration of the remote sensing-based product with the NF&WI data; and finally iv) compared the precision of the map-assisted estimates to the precision of the field-based AGB estimates from the NF&WI. Four scenarios are considered. In the baseline scenario A, the (sub)national AGB estimates correspond to simple expansion estimates using only the NF&WI data; for scenarios B-D, we introduced the European Space Agency Climate Change Initiative (CCI) (Santoro and Cartus, 2021) biomass map as auxiliary data. In scenario B, we used the aforementioned map in its published form; while for scenarios C-D we

first locally calibrated the biomass map using the plot data and a linear regression model. In scenario D we used hybrid inferential techniques to additionally account for the effects of measurement variability, geolocation error and the uncertainties owing to the plots covering smaller areas than the remote sensing-based sampling units (here-after characterized as within-block variability). We argue that by accounting for the uncertainties from all the sources, we produce more comprehensive map-assisted AGB uncertainty estimates and thereby better comply with the IPCC good practice guidelines (Eggleston et al., 2006, Vol 1, Chap 1, Section 1.2).

2. Material and methods

2.1. The biomass map

We used the 2017 v.3 CCI global AGB biomass map (Santoro and Cartus, 2021) as auxiliary data. The map has a 100 m resolution and its nominal date is closest to the NF&WI implementation period and, therefore, minimizes potential differences caused by temporal mismatches (GFOI, 2020). The map was developed by combining Synthetic Aperture Radar (SAR) C-band Sentinel-1 information and Phased Array L-band SAR (PALSAR-2) data from ALOS-2 as well as other auxiliary data (Santoro and Cartus, 2021). The map processing chain first predicts growing stock volume, which is next converted to AGB predictions at approximately 100 m resolution by means of biomass conversion and expansion factors.

2.2. Defining the population

Our population is defined in accordance with Peru's NF&WI survey. Of the six subpopulations defined by the NF&WI (hereafter characterized as strata), the four strata within Amazonia pertain to our research. They are defined as hydromorphic zone (HZ), accessible montane forest (AMF), inaccessible montane forest (IMF) and lowland forest (LF) strata. More on the NF&WI stratification information is included in Supplemental Material S.1. The Peruvian survey concerns only forested areas according to a preliminary remote sensing-based land cover assessment (MINAGRI and MINAM, 2016). Hence, our population is constrained to the Peruvian Amazonia forestland.

The NF&WI uses a non-aligned systematic sampling design with plots randomly located within coarse grid cells whose sizes differ per stratum (20–34 km) (MINAGRI and MINAM, 2016). All coarse grid cells were assigned to panels based on accessibility and similar criteria to facilitate the work of the field-crew and to reduce costs. In total, there are five panels uniformly distributed throughout each stratum. By the time of our analysis, plots in approximately two of the panels, hereafter designated panel 1 and panel 2, had been measured. A few plots within these panels were missing and were considered missing at random. For the purpose of this study, coarse grid cells assigned to panels 1 and 2 within the Peruvian Amazonia forestland defined the population (Fig. 1). Population units are either 4x4 or 5x5 (depending on the stratum) blocks of aggregated CCI pixels.

Within the HZ, AMF and IMF strata, plots consist of 10 circular subplots (0.05 ha), while in the LF stratum they consist of seven rectangular subplots (0.1 ha). In all strata, the subplots are arranged in L-shaped configurations (Fig. 2a and 2b). The length of the edges of the population units (square blocks of pixels) approximates the length of the longest arm of the NF&WI plot (Fig. 1).

The sample consisted of blocks enclosing the field plots. We recreated N-S and E-W orientated map blocks (of size ~ 400 m × 400 m and ~ 500 m × 500 m, depending on the stratum), where the southwest corner was located 50 m south and 50 m west of each plot anchor point (Fig. 1). The AGB observation for the ith sample unit in the hth stratum, hereafter denoted y_{hi}, is the AGB mean over the seven or 10 subplots of the plot located in the ith sample unit. The corresponding sample unit map value, hereafter denoted $\hat{y}_{hi}$, is the AGB mean over the 4x4 or 5x5
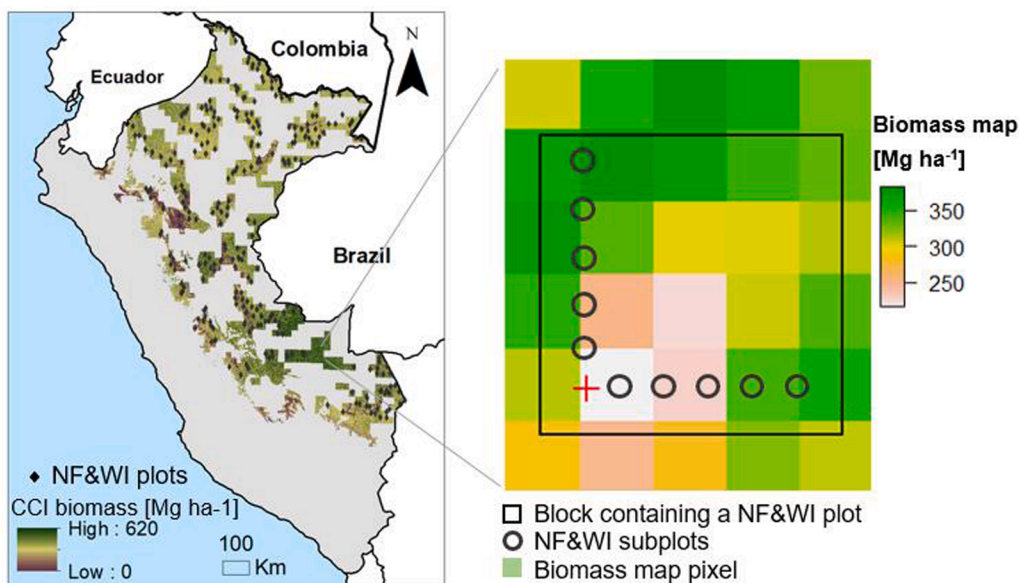
Fig. 1. CCI biomass map for panels 1 and 2 within the Peruvian Amazonia. On the right, an example of a plot roughly covering a block of 4x4 map pixels. The red cross is the plot's anchor point. (For interpretation of the references to colour in this figure legend, the reader is referred to the web version of this article.)
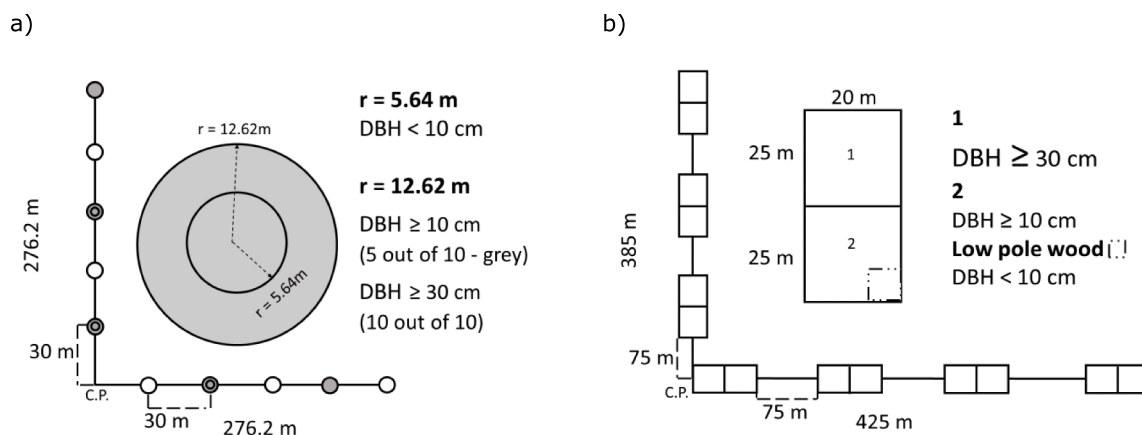

Fig. 2. (a) Plot configuration of the HZ, AMF and the IMF strata. (b) Plot configuration of the LF stratum. Adapted from MINAGRI and MINAM (2016).

CCI pixels defining the ith sample unit.

2.3. Field-based AGB

Our analysis included live-woody AGB information for 299 plots (32 in HZ; 46 in AMF; 11 in IMF and 210 in LF). The inventory data were mostly provided at tree level and included information such as subplot coordinates, diameter at breast height (DBH) for trees with DBH $\geq$ 10 cm and wood density (WD). The plot-level AGB and corresponding measurement errors were estimated using the approach of Réjou-Méchain et al. (2017) as implemented in the BIOMASS R package. Plot-level AGB estimates and pre-processing activities are addressed in Supplemental Material S.1.

2.4. Map harmonization

Our pre-processing and data harmonization steps included:

i. *Re-projection.* We made sure that the plot coordinates, the biomass map and auxiliary information were in the WGS 1984/ UTM zone 18S projection system.

ii. *Map pixel size harmonization.* The 2016 land-use mask of Peru (Plataforma Geobosques, 2021) was resampled to the same pixel size as the biomass map ($\sim$100 m $\times$ 100 m) by majority (mode). This mask was used to define the population of forested pixels.

iii. *Cropping and masking:* We cropped the biomass map to the extent of panels 1 and 2 within the Peruvian Amazonia. Additionally, we used the re-sampled land-use mask of Peru to mask all non-forest pixels from the biomass map.

The mean AGB map block values were calculated by ignoring any non-forest (NA) pixels.

2.5. Statistical estimators

In scenario A, we used the simple expansion estimator directly with the NF&WI plot data. In the other scenarios (B-D), the biomass map was introduced as auxiliary information and used with model-assisted estimators (Table 1).

2.5.1. Scenario A: Field-based estimation (Baseline)

In our baseline scenario, only the plot-based AGB data as described in section 2.3 and Supplemental Material S.1 were used. To compute the

Table 1
Summary of scenarios A-D.

	A	B	C	D
Inferential strategy	Design-based	Design-based model assisted estimation		Hybrid inference
Use of the biomass map as a source of auxiliary information	No	Yes, in its original form	Yes, locally calibrated using the NF&WI data	
Statistical estimators	Simple expansion estimator	Model-assisted difference estimator	Model-assisted regression estimator	Model-assisted regression estimator within an hybrid approach
Accounting for the effects of the measurement, geo-location and within block uncertainty	No	No	No	Yes

per-stratum AGB estimates, we used the simple expansion estimator, assuming the plots were a probabilistic random sample of the stratum (McRoberts et al., 2020):

$$\widehat{\mu}_h = \frac{1}{m_h} \sum_{i=1}^{m_h} y_{hi} \tag{1}$$

where m_h is the number of plots in stratum h, and y_{hi} is the AGB mean over the seven or 10 subplots of the plot located in the ith sample unit.

The variance estimator is defined as:

$$\widehat{VAR}(\widehat{\mu}_h) = \frac{1}{m_h(m_h - 1)} \sum_{i=1}^{m_h} (y_{hi} - \widehat{\mu}_h)^2. \tag{2}$$

2.5.2. Map-assisted scenarios B - D: Using the biomass map as auxiliary data for the per stratum estimation

The model-assisted estimators of the population mean and variance were similar for the scenarios B-D. In scenario B, the AGB predictions of the population units, $\widehat{y}_{hj}$, correspond to AGB means over the 4x4 or 5x5 uncalibrated CCI map values. In scenarios C and D the AGB predictions, $\widehat{y}_{hj}$, are AGB means over the 4x4 or 5x5 values of the map calibrated using a regression model fitted to the plot data (section 2.6).

The difference (scenario B) and the regression estimators (scenario C and D) of the population mean consist of the sum of a predictions-based term and a residuals-based adjustment term. Using remotely sensed auxiliary data, the within-stratum prediction-based term is the synthetic estimate ($\widehat{\mu}_h syn$) calculated as the mean of predictions ($\widehat{y}_{hj}$) over all population units (Särndal et al., 1992, p.222). The within-stratum adjustment term is based on differences between sample unit observations (y_{hi}) and their corresponding sample unit map values ($\widehat{y}_{hi}$). Hence, the within-stratum estimator is (Lohr, 2010, Section 5.1):

$$\widehat{\mu}_h = \frac{1}{M_h} \sum_{j=1}^{M_h} \widehat{y}_{hi} + \frac{1}{m_h} \sum_{i=1}^{m_h} \varepsilon_{hi} \tag{3}$$

where j indexes the population units within stratum h, M_h is the number of population units in stratum h, m_h is the number of sample units in stratum h and the sample unit residuals ε_{hi} are calculated as, $\varepsilon_{hi} = y_{hi} - \widehat{y}_{hi}$.

The within-stratum variance estimator (Lohr, 2010, Section 5.1) is:

$$\widehat{VAR}(\widehat{\mu}_h) = \frac{1}{m_h(m_h - 1)} \sum_{i=1}^{m_h} (\varepsilon_{hi} - \bar{\varepsilon}_h)^2 \tag{4}$$

$$\bar{\varepsilon}_h = \frac{1}{m_h} \sum_{i=1}^{m_h} \varepsilon_{hi}$$

2.5.3. Peruvian Amazonia forest-related AGB estimation

For all scenarios, we used post-stratified estimators for our across-strata population estimates (Næsset et al., 2020):

$$\widehat{\mu} = \sum_{h=1}^{H} \frac{M_h}{M} \widehat{\mu}_h \tag{5}$$

$$\widehat{VAR}(\widehat{\mu}) = \sum_{h=1}^{H} \left(\frac{M_h}{M}\right)^2 \widehat{VAR}(\widehat{\mu}_h) \tag{6}$$

where M refers to the population size across all strata ($M = 1\ 578\ 357$)

We estimated the per-stratum and Amazonia level gain in precision from the contribution of the biomass map by means of relative efficiency (RE), a ratio that compares the variance estimated in senario A ($\widehat{VAR}(\widehat{\mu})_{field}$) and the variance from our map-assisted estimates from scenarios B-D ($\widehat{VAR}(\widehat{\mu})_{map}$)(Næsset et al., 2020).

$$RE = \frac{\widehat{VAR}(\widehat{\mu})_{field}}{\widehat{VAR}(\widehat{\mu})_{map}} \tag{7}$$

2.6. Calibrating the biomass map

For scenarios C and D, and within each stratum h, we fitted simple linear regression models to predict AGB (Mg ha^{-1}) for each map unit, thereby constructing a new locally calibrated map. In scenario C, we established a regression model where the sample unit observations (y_{hi}) are the dependent (response) variable and the sample unit map values ($\widehat{y}_{hi}$) are the independent (predictor) variable. The parameters β_{h0} and β_{h1} are to be estimated and $\varepsilon_i\ N(0, \sigma_i^2)$.

$$y_{hi} = \beta_{h0} + \beta_{h1} * \widehat{y}_{hi} + \varepsilon_{hi} \tag{8}$$

Four AGB plot estimates within the LF forest stratum were not representative of the subpopulation and therefore excluded when fitting the regression models for both scenarios, but they were included when estimating means and variances. These four plots included very large trees (larger than any trees reported in Chave et al. (2014)) within very small plots and therefore resulted in questionable plot-based AGB ha^{-1} for Amazonian lowland forests.

Scenario D additionally accommodated the effects of different sources of uncertainty involved in map-to-plot comparisons. In this scenario, regression models (Eq. (9)) were fitted to the residuals between sample unit map values ($\widehat{y}_{hi}$) and AGB values obtained by Monte Carlo simulations that account for measurement variability ($y_{hi}^k M.V$), geo-location error ($y_{hi}^k L.E$) and the within-block variability ($y_{hi}^k WB.V$), which are further addressed in section 2.7. In each Monte Carlo run (indexed by superscript k), a set of simulated values for $y_{hiM.V}^k y_{hiL.E}^k$, $y_{hiWB.V}^k$ for the ith sample unit was generated. Hence, model parameters β_{h0}^k and β_{h1}^k were estimated in that run and used to predict AGB values (section 2.7). Unlike Eq. (8), the model was fitted to the residuals, because the within-block variability is estimated as the difference between AGB averaged over subplot locations within a plot and $\widehat{y}_{hi}$. For all models, the residuals were tested for heteroscedasticity using the Breusch-Pagan test Zeileis and Hothorn, 2002. <1% of runs had $p < 0.05$, for most strata. Even in the LF stratum where the percentage was greater, the correction for heteroscedasticity had a negligible effect on our estimates. The regression approach used in each Monte Carlo realization, k, is described by Eq. (9).

$$\left(y_{hiM.V}^k - \widehat{y}_{hi}\right) + \left(y_{hiL.E}^k - \widehat{y}_{hi}\right) + \left(y_{hiWB.V}^k\right) = \beta_{h0}^k + \beta_{h1}^k * \widehat{y}_{hi} + \varepsilon_{hi}^k \tag{9}$$

2.7. Accounting for the sources of uncertainty from the integration of the biomass map with the plot data (scenario D)

We used hybrid inferential methods to estimate per stratum and overall population estimates of AGB and their variances by propagating the effects of the sources of uncertainty associated with the allometric model predictions, geo-location error and the within-block variability as well as the contribution from the designed-based sampling variability. We used a Monte Carlo simulation procedure with 1000 runs as described by McRoberts et al. (2016) to combine the model-based prediction uncertainty and probability-based sampling variability.

2.7.1. Measurement variability ($y_{hi}^k M.V$)

We used the *AGBmonteCarlo* function available in *BIOMASS* (Réjou-Méchain et al., 2017) to propagate the uncertainties associated with the measurement of DBH, WD and the Chave et al. (2014) generalized allometric model parameters and residuals. We predicted tree-level AGB similarly to the previous scenarios (Supplemental Material S.1), but additionally accounted for the aforementioned uncertainties using the Monte Carlo scheme available in Réjou-Méchain et al. (2017). We simulated 1000 AGB values for subplots which were averaged to the plot-level ($y_{hi}^k M.V$) and extracted from the map-based AGB ($\widehat{y}_{hi}$) to calculate the residuals in the left-hand side of Eq. (9).

2.7.2. Geo-location error ($y_{hi}^k L.E$)

Ground-based data with geo-referencing errors are prone to mismatches when integrated with remote sensing-based products with the errors affecting the map-assisted estimates of mean AGB (Mg ha^{-1}). The NF&WI reported maximum GPS location errors of 10, 25, 25 and 30 m for the HZ, LF, IMF and AMF strata, respectively. We modelled the effect of the plot geo-location error by simulating 1000 potential plot anchor point locations from a uniform random angle between a 0–2 π and maximum radius equivalent to the per stratum GPS error (Fig. 3b). Hence, we obtained 1000 simulated blocks and estimated the corresponding map AGB weighted mean values $y_{hi}^k L.E$ (Fig. 3a), which were later subtracted from the estimated map-based AGB ($\widehat{y}_{hi}$).

2.7.3. Within-block variability ($y_{hiWB.V}^k$)

In general, the area represented by a large-scale biomass map pixel is far greater in size than an NFI plot. Therefore, local forest biomass spatial variability can contribute to uncertainties when pairing the map information and the plot data (Réjou-Méchain et al., 2014). Here, we

applied a geostatistical approach to model the forest biomass distribution within our map-based blocks containing the L-shaped NF&WI plot configuration (Gotway and Young, 2002; Kyriakidis, 2004). We assessed within-block variability by simulating differences between the AGB averaged over subplot locations within a plot and the map-based AGB within blocks. We implemented the following procedure within each stratum:

i) We estimated semi-variances from all available ground-based subplots within the stratum in log-transformed AGB and fit variogram functions using the *gstat* package for R (Gräler et al., 2016). The mean measurement variability (also transformed to log scale) was subtracted from the nugget as described by Christensen (2011) thereby avoiding double counting of the measurement variability in our regression model (Eq. (9)). The variogram models are shown in detail in the Supplemental Material S.2.
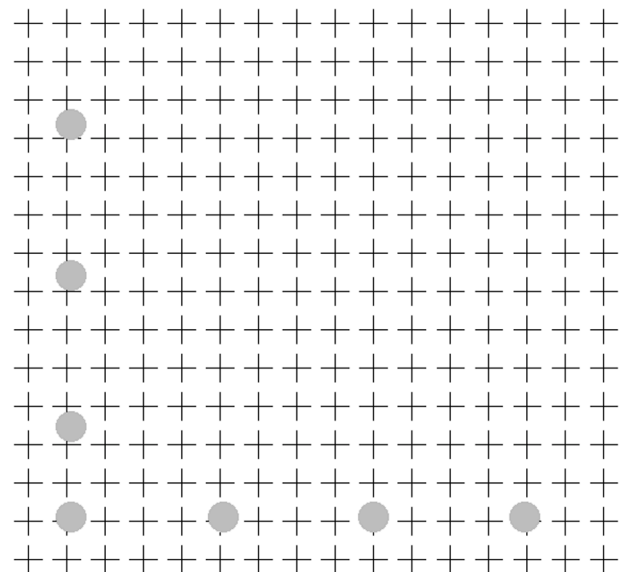

Fig. 4. Block discretized into locations with subplot support (+) and seven subplot locations forming an L-shaped plot configuration () within the LF stratum.
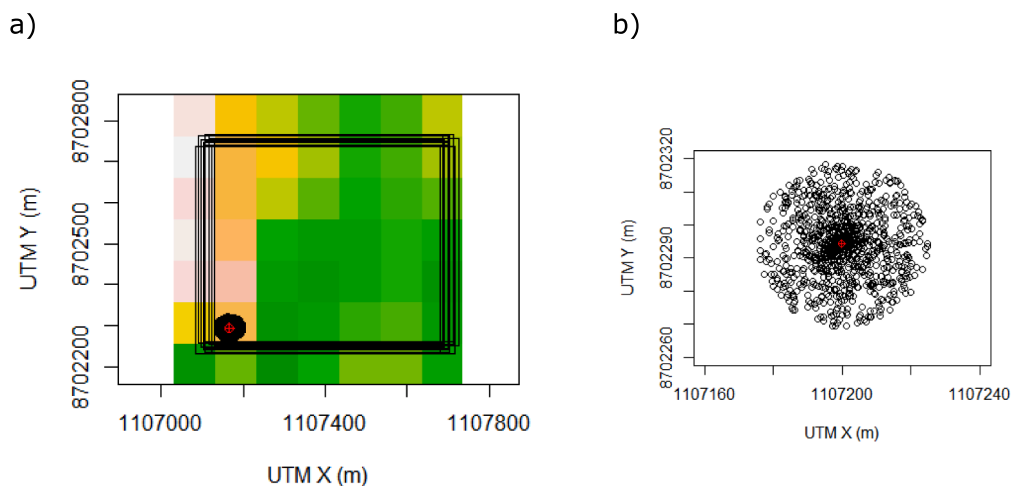
a)   b)

Fig. 3. (a) CCI biomass map and 12 of the 1000 sample unit realizations in the LF stratum. The distribution of the simulated plot anchor point locations (in black) and recorded location (red cross) are detailed in (b). (For interpretation of the references to colour in this figure legend, the reader is referred to the web version of this article.)

ii) The map-based block was discretized by points (Fig. 4 – crosses). The discretization grid corresponds to the centres of a tessellation of the block by square plots having the size of the subplots.

iii) Using a Monte Carlo approach, we simulated log(AGB) at each grid node within the block using the variogram model obtained in step i). The simulated log(AGB) values at each individual grid node were back-transformed by exponentiation, which was followed by a multiplicative correction to force the average over the within-block locations to match the AGB map value of the block $(\widehat{y}_{hi})$.

iv) For each ith sample unit and k^th iteration, we calculated the mean over the simulated (back-transformed) AGB predictions at the grid nodes corresponding to the 7–10 subplots locations within the L-shaped plot configuration and subtracted the map-based block values $(\widehat{y}_{hi})$ to obtain the within-block residuals expressed in Eq. (9) $(y_{hi}^{k} WB.V)$.

2.7.4. Simulation procedure and mean AGB

The effects of the three previously described sources of uncertainty on the mean calibrated AGB were assessed by Monte Carlo simulations as described by McRoberts et al. (2016). For each kth simulation

(replications k = 1, 2, ……., 1000):

i) We fit regression models (Eq. (9)) to the residuals of the simulated AGB observations $(y_{hi}^{k} M.V, y_{hi}^{k} L.E$ and $y_{hi}^{k} WB.V)$ and the map-based $(\widehat{y}_{hi})$ values, and then used the resulting model parameter estimates to calculate the AGB predictions for each ith sample unit $(\widehat{y}_{hi}^{k})$.

ii) To estimate the per stratum mean AGB (Mg ha^{-1}) $(\widehat{\mu}_{h}^{k})$ and corresponding variance $(\widehat{VAR}(\widehat{\mu}_{h}^{k}))$ within the simulations, we used the model-assisted estimators defined in section 2.5 (Eqs (3 and (4)) where $\widehat{y}_{hj}^{k}$ are the population unit AGB predictions from our calibrated map .

The per stratum AGB mean $(\widehat{\mu}_{h}^{k})$ and variance $(\widehat{VAR}(\widehat{\mu}_{h}^{k}))$ were estimated using Eqs 10 and 11, respectively:

$$\widehat{\mu}_{h} = \frac{1}{1000} \sum_{k=1}^{1000} \widehat{\mu}_{h}^{k} \qquad (10)$$

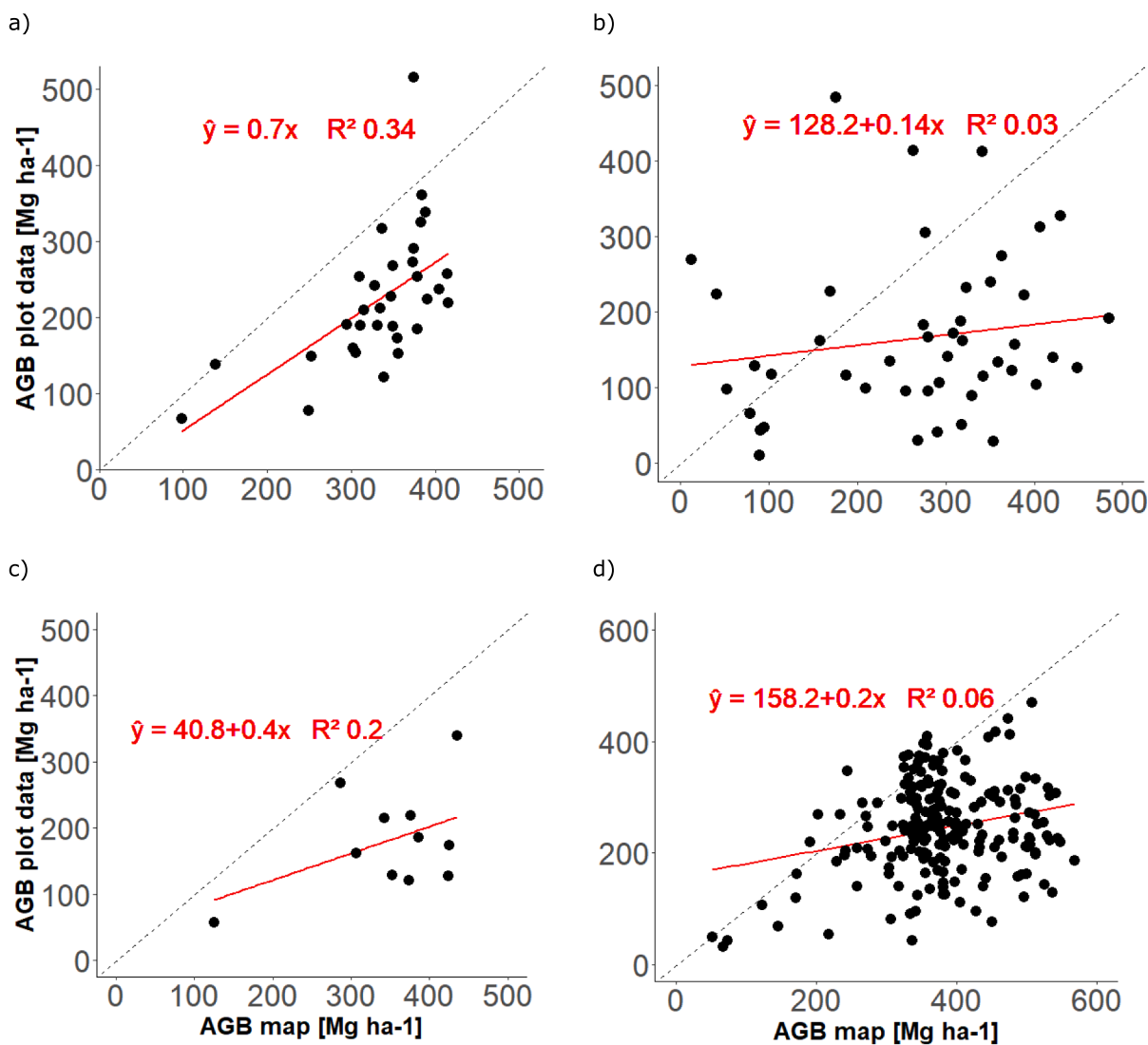$$\widehat{VAR}(\widehat{\mu}_{h}) = \left(1 + \frac{1}{1000}\right) * W_{1} + W_{2} \qquad (11)$$

Fig. 5. Relationship between the map-based AGB values and observed NF&WI values for HZ (a), AMF (b), IMF (c), and LF (d) strata. The scenario C regression models to calibrate the biomass map and the correspondent equations are shown in red, the dashed grey line is the 1:1 line. (For interpretation of the references to colour in this figure legend, the reader is referred to the web version of this article.)

where $W_1 = \frac{1}{1000}\sum_{k=1}^{1000}(\widehat{\mu}_h^k - \widehat{\mu}_h)$ refers to the among replications variance and $W_2 = \frac{1}{1000}\sum_{k=1}^{1000}\widehat{VAR}(\widehat{\mu}_h^k)$ is the mean within replications variance. Finally, we used Eqs. (5) and (6) for estimating the overall Peruvian Amazonia mean AGB (Mg ha^{-1}).

3. Results and discussion

3.1. Locally calibrating the large-area biomass map

For all four strata within the Peruvian Amazonia, the CCI biomass map tends to overestimate AGB when compared to our plot data, most evidently for small AGB values (Fig. 5). For scenario C, two of the four per stratum linear regression models were significant (p < 0.001), although all had small coefficients of determination (R^2 0.02–0.3) (Fig. 5). For the accessible and inaccessible montane forest strata (Fig. 5b and c), the regression models were non-significant (p > 0.05), attributable to large trees within small subplots and to the small sample sizes within these strata. Additionally, only 11 plots were available for the IMF stratum, thereby detracting from the statistical rigor of our analysis, which may change once the NF&WI progresses in its implementation. We selected a non-intercept linear model in the HZ stratum for both scenarios to avoid negative AGB map values after calibration. In scenario D, we fit the regression model (Eq. (9)) within a Monte Carlo approach to account for the measurement variability, geo-location and within-block variability. R^2 varied between 0 and 0.7 for all strata, with the HZ stratum having the smallest values. Most models for the IMF stratum and HZ, were not statistically significant at the 95% significance level.

In global validation, large-scale biomass maps tend to overestimate small biomass and underestimate large biomass plot values (>150 Mg ha^{-1}), a trend from which CCI biomass products are not exempt (Avitabile et al., 2016). However, the global map-plot comparison pattern can have local exceptions, as shown in the map-based biomass overestimation in our case study (e.g. Fig. 5a). Additionally, Réjou-Méchain et al. (2019) compared several biomass maps available for the pantropics (including the CCI biomass map) against fine resolution biomass products and also found weak coefficients of determination (R^2 < 0.3).

3.2. Addressing the sources of uncertainty

Consistently among strata, the within-block variability and geo-location error were the largest and the smallest contributors, respectively, to the overall uncertainty resulting from the integration of the CCI biomass map and the NF&WI plot data. The standard deviation of measurement variability fluctuated between 27 and 38 Mg ha^{-1} among strata, whereas the within-block variability ranged between 72 and 90 Mg ha^{-1} (Fig. 6). Similar to other studies, the contribution of the geo-
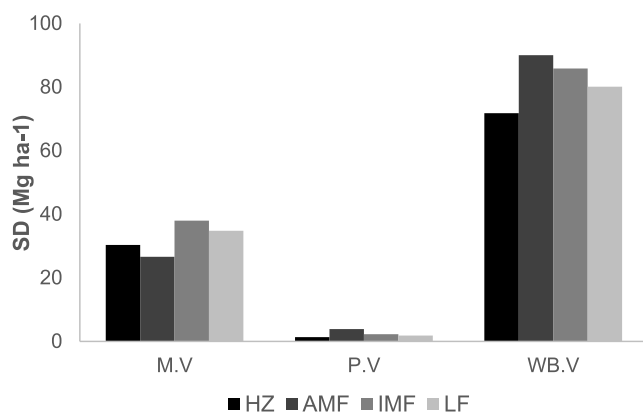

Fig. 6. Per stratum standard deviations (SD) due to measurement variability (M.V), geo-location error (L.E), and within-block variability (WB.V).

location error was negligible (McRoberts et al., 2002).

Plot AGB values are allometric model predictions rather than error-free observations but uncertainties associated with plot data are usually ignored in AGB monitoring and reporting. Systematic errors associated with the prediction of WD and the application of allometric models might have large effects at the population level in the tropics due to adverse conditions (i.e. inaccurate species identification, limited information of WD database, presence of very large trees, etc.) (Réjou-Méchain et al., 2019; Ståhl et al., 2014; Chave et al., 2014). Our results are consistent with a study in temperate forests that also used hybrid inference to address the effects of allometric model prediction uncertainty on map-assisted AGB estimates (McRoberts et al., 2016). The greatest contribution to the measurement variability from the IMF and LF stratum can be attributed to very large trees within small plots.

Previous studies have shown the effects of differences in the remote sensing spatial support and plot size on capturing local AGB spatial variability; within pixel AGB variability is larger when the pixel-to-plot ratio also increases (Réjou-Méchain et al., 2019, 2014; Saatchi et al., 2011). We modelled the AGB variability within blocks of size ~ 16 ha and 25 ha by means of a geostatistical approach using variograms estimated from data for small subplots. Like other studies in the neotropics that stressed the large spatial variability of forest structural metrics over short distances (Chave et al., 2004, 2003; Saatchi et al., 2011), we found large AGB heterogeneity within our blocks. Within the two most data-rich strata (AMF and LF, Supplemental Material S. 2), the ranges of spatial correlations varied from 15 to 30 km. Still, the large nugget-to-sill ratio of our variograms shows that most variability in AGB occurs at very short distances (<30 or 75 m).

The major contribution of the within-block variability found in this study indicates that the small plot size within larger map-based sampling units is the main source of uncertainty in map-plot comparisons. The advantage of large, single plot configurations as opposed to plots with small subplots has been stressed in literature, because small plots are prone to introduce errors related to mismatches in the sampling area, edge effect, measurement errors, etc. (Chave et al., 2004; Réjou-Méchain et al., 2014, 2019; Ploton et al., 2020). However, the large costs of establishing a plot in the tropics have favoured the use of NFI plot configurations involving small subplots. Foreseeing the increasing contribution of open-source remote sensing-based products for national and subnational forest-related estimation and management, future work should assess the contribution of remote sensing-based products under different NFI plot configurations, how well the spatial plot configuration captures local AGB variability and ultimately, how the configuration affects the precision of the estimates (Næsset et al., 2020).

3.3. Increased precision of subnational AGB estimates

Mean forest AGB estimates at stratum level using only the NF&WI data (scenario A) ranged between 165 and 253 Mg ha^{-1} among strata (Table 2). In a preliminary report, SERFOR stated AMF: 145.4 Mg ha^{-1}; IMF: 166.5 Mg ha^{-1}, LF: 295.4 Mg ha^{-1}, HZ:188.6 Mg ha^{-1}; no standard errors were reported (SERFOR, 2020). Differences from our results may be attributed to the NF&WI estimates being based on a smaller sample (approximately half of the sample used in this study), as well as the application of different allometric models (i.e., species-specific models) and the inferential approach.

Model-assisted estimation using the uncalibrated biomass map to adjust for systematic map errors ($\widehat{\mu}_h syn$) considerably overestimated mean forest-related AGB stocks for all strata (scenario B - Table 2). These systematic errors reveal that this global biomass map is not directly suitable for national or subnational AGB estimation and GHG reporting schemes, which concurs with a study for African dry forests and woodlands (Næsset et al., 2020).

Our results show that introducing the map as a source of auxiliary information slightly increased the precision of our AGB map-assisted estimates. Without local calibration, the standard errors (SEs) in

Table 2

Stratum-wise and Peruvian Amazonia sample size (n), mean AGB ha^{-1} ($\widehat{\mu}_h$) and standard error (SE) estimates (Mg ha^{-1}), as well as relative efficiency (RE) indicator.

Strata	n	Scenario A		Scenario B				Scenario C				Scenario D			
		$\widehat{\mu}_h$	SE	$\widehat{\mu}_h syn$	$\widehat{\mu}_h$	SE	RE	$\widehat{\mu}_h syn$	$\widehat{\mu}_h$	SE	RE	$\widehat{\mu}_h syn$	$\widehat{\mu}_h$	SE	RE
HZ	32	223.8	15.6	323.0	213.6	13.0	1.4	217.8	216.9	12.6	1.5	225.8	222.9	14.9	1.1
AMF	46	165.3	15.7	243.6	140.8	21.9	0.5	161.9	161.9	15.5	1.0	165.7	165.9	15.8	1.0
IMF	11	181.5	23.4	340.2	173.3	26.1	0.8	178.2	178.2	20.8	1.3	186.8	186.6	25.3	0.9
LF	210	253.5	7.2	384.5	262.5	9.1	0.6	246.4	255.5	7.2	1.0	246.9	255.9	7.5	0.9
Amazonia	299	218.9	6.9		215.8	8.1	0.7		211.0	6.4	1.2		221.1	7.2	0.9

*$\widehat{\mu}_h syn$ stands for synthetic estimator.

scenario B mostly showed no reduction in comparison to our baseline scenario A (Table 2). However, after calibrating the biomass map (scenario C), most strata (except for the LF forest) presented a gain in precision, as indicated by smaller SEs in comparison to scenario A. The gain in precision of our estimates can be explained by the RE indicator (Eq. (7), Table 2). For instance, relative to the simple expansion estimates, a RE value of 1.2 (scenario C – Amazonia level) represents a gain in precision of 20%, meaning that 1.2 times more plots would be needed by the NF&WI to reach the same level of precision as the current model-assisted AGB estimates (McRoberts et al., 2014). Within strata, the precision increased by as much as 50%. After propagating the effects of the sources of uncertainty (scenario D), SEs marginally changed in comparison to scenario A, ranging from 7.5 to 25.3 Mg ha^{-1} among strata. The precision of our Amazonia level estimates actually decreased by 10% (Table 2). For most strata, differences in SEs between our baseline and map-assisted estimates were only evident in scenario C, revealing the contribution of the local calibration of the global map. However, scenario D provides the most comprehensive and transparent representation of the map-assisted AGB estimation.

Previous studies have shown how the use of remote sensing-based products as sources of auxiliary information can support AGB estimates for GHG monitoring and reporting (McRoberts et al., 2020; Ogle et al., 2019). Nonetheless, few studies have reported the application of global biomass products to enhance inferences for national or subnational AGB estimates, particularly in humid tropical forests. Studies in dry tropical forests and temperate forests have shown marginal precision gain of model-assisted AGB estimates when uncalibrated maps are used as an auxiliary source of information, but found substantial improvements when using locally calibrated global products (Næsset et al., 2020; McRoberts et al., 2019). Our results partially agree with the aforementioned studies, although the gain in precision of our map-assisted estimates in scenario C is smaller. These former studies do not account for the effects of the sources of uncertainty affecting the integration of plot and map biomass products, as we did in our scenario D. We stress the relevance of accounting for these uncertainties, especially the within-block variability whose contribution was found to be at least three times greater than the other two. By doing so, we assess the contribution of a large-area biomass product to (sub)national map-assisted AGB estimates more comprehensively, complying with IPCC guidelines on accounting for sources of uncertainty (Eggleston et al., 2006, Vol 1, Chap 1, Section 1.2). Further case studies on the contribution of biomass products to (sub)national estimates under different biomass densities, especially within tropical humid forests, is encouraged.

The small correlations found between the NF&WI plots and our CCI biomass map blocks limited the gain in precision of Peru's (sub)national AGB estimates. As addressed by Næsset et al. (2016) in Miombo woodlands, finer spatial resolution remote-sensing products (i.e., derived from ALS or RapidEye) enhanced the precision of AGB estimates threefold when compared with global products. Nonetheless, the effort and capacity needed within tropical countries to process nation-wide openly available fine resolution, remote sensing-based products for enhancing AGB national estimates are much larger than when using an existing biomass product. Global biomass products are encouraged to be used in the context of GHG accounting and reporting if they are well-calibrated to national circumstances (Ogle et al., 2019). As efforts in mapping biomass improve, more accurate maps imply greater correlations and hence more favourable conditions for further increasing the precision of national AGB estimates.

Increasing the statistical precision of AGB estimates with auxiliary information suggests that either the target level of precision for AGB can be met with fewer plots or the original target level of precision can be exceeded with the original sample size (McRoberts et al., 2002). Our study is especially relevant for Peru's monitoring efforts, because only 10–35% of the per-stratum target sample had been accomplished by 2020, mostly due to budget constraints. We here present a reproducible method that countries can benefit from. As the accuracy of global biomass products continues to evolve, their contribution to enhancing the precision of country AGB estimates will, likewise, increase over time. As for the case of Peru, once the NF&WI implementation progresses, the contribution of the biomass maps products to the precision of their (sub) national estimates could also be benefited once more field-based information becomes available.

4. Conclusions

We found that without calibrating the map to correct for the systematic map error, the 2017 CCI biomass map tends to overestimate forest-related AGB values across Peruvian Amazonia, revealing that there is room for improvement for AGB stocks to be estimated directly from large-area biomass maps.

Addressing the sources of uncertainties promotes more accurate and transparent AGB estimation, which translates to more credible country GHG reporting practices. We found that the within-block AGB variability was the largest contributor among the propagated sources of uncertainty. It affects plot-map integration because NFI plot data are often acquired over smaller spatial units than the remote sensing-based sampling units and strongly contributes to the non-negligible uncertainty of plot AGB data. In contrast, the contribution of the geo-location error was virtually negligible. Our study shows that accounting for error sources and propagating uncertainties resulting from integration of plot- and space-based biomass information is possible. We rigorously estimated the uncertainties, providing subnational AGB estimates that comply with the IPCC good practice guidelines.

Using a global biomass map as a source of auxiliary information with the NF&WI reference data led to a small increase in the precision of forest-related per stratum estimates and Peruvian Amazonia AGB map-assisted estimates. After calibration, the map slightly increased the precision of the AGB estimates, which was constrained by the small map-plot correlations. However, when propagating the aforementioned sources of uncertainty, the map no longer contributed to increasing the precision. As the main source of uncertainty is attributed to the plot size being smaller in size than the remote sensing-based sampling units, we encourage the expansion of this work to explore the contribution of biomass maps to (sub)national AGB estimates under a range of AGB settings and capturing a cross-country diversity of sampling designs and

plot configurations. We present a reproducible method that countries can build upon and further improve while the biomass map products continue to improve over time. Further improvement of space-based biomass products should enhance their usefulness for enhancing (sub) national AGB estimates and other applications beyond than addressed in this study.

CRediT authorship contribution statement

Natalia Málaga: Conceptualization, Methodology, Data analysis. **Sytze de Bruin:** Conceptualization, Methodology. **Ronald E. McRoberts:** Conceptualization, Methodology. **Alexs Arana Olivos:** Data collection, Analysis. **Ricardo de la Cruz Paiva:** Data collection, Analysis.. **Patricia Durán Montesinos:** Data collection, Analysis. **Daniela Requena Suarez:** Data analysis. **Martin Herold:** Conceptualization, Methodology.

Declaration of Competing Interest

The authors declare that they have no known competing financial interests or personal relationships that could have appeared to influence the work reported in this paper.

Data availability

The authors do not have permission to share data.

Acknowledgements

Appendix A. Supplementary data

Supplementary data to this article can be found online at https://doi.org/10.1016/j.jag.2022.103102.

References

Avitabile, V., Herold, M., Heuvelink, G.B.M., Lewis, S.L., Phillips, O.L., Asner, G.P., Armston, J., Ashton, P.S., Banin, L., Bayol, N., Berry, N.J., Boeckx, P., de Jong, B.H. J., DeVries, B., Girardin, C.A.J., Kearsley, E., Lindsell, J.A., Lopez-Gonzalez, G., Lucas, R., Malhi, Y., Morel, A., Mitchard, E.T.A., Nagy, L., Qie, L., Quinones, M.J., Ryan, C.M., Ferry, S.J.W., Sunderland, T., Laurin, G.V., Gatti, R.C., Valentini, R., Verbeeck, H., Wijaya, A., Willcock, S., 2016. An integrated pan-tropical biomass map using multiple reference datasets. Glob. Change Biol. 22, 1406–1420. https://doi.org/10.1111/gcb.13139.
Chave, J., Condit, R., Aguilar, S., Hernandez, A., Lao, S., Perez, R., 2004. Error propagation and scaling for tropical forest biomass estimates. Philos. Trans. R. Soc. Lond. B. Biol. Sci. 359, 409–420. https://doi.org/10.1098/rstb.2003.1425.
Chave, J., Condit, R., Lao, S., Caspersen, J.P., Foster, R.B., Hubbell, S.P., 2003. Spatial and temporal variation of biomass in a tropical forest: results from a large census plot in Panama. J. Ecol. 91, 240–252. https://doi.org/10.1046/j.1365-2745.2003.00757.x.
Chave, J., Réjou-Méchain, M., Búrquez, A., Chidumayo, E., Colgan, M.S., Delitti, W.B.C., Duque, A., Eid, T., Fearnside, P.M., Goodman, R.C., Henry, M., Martínez-Yrízar, A., Mugasha, W.A., Muller-Landau, H.C., Mencuccini, M., Nelson, B.W., Ngomanda, A., Nogueira, E.M., Ortiz-Malavassi, E., Pélissier, R., Ploton, P., Ryan, C.M., Saldarriaga, J.G., Vieilledent, G., 2014. Improved allometric models to estimate the aboveground biomass of tropical trees. Glob. Change Biol. 20, 3177–3190. https://doi.org/10.1111/gcb.12629.

Christensen, W.F., 2011. Filtered Kriging for Spatial Data with Heterogeneous Measurement Error Variances. Biometrics 67, 947–957. https://doi.org/10.1111/j.1541-0420.2011.01563.x.
Eggleston, H.S., Buendia, L., Miwa, K., Ngara, T., Tanabe, K. (Eds.), 2006. 2006 IPCC guidelines for national greenhouse gas inventories. National greenhouse gas inventories programme. IGES, Japan.
GFOI, 2020. Integration of remote-sensing and ground-based observations for estimation of emissions and removals of greenhouse gases in forests: Methods and guidance from the Global Forest Observations Initiative., 3.0. ed. U.N. Food and Agriculture Organization, Rome, Italy.
Gotway, C.A., Young, L.J., 2002. Combining Incompatible Spatial Data. J. Am. Stat. Assoc. 97, 632–648. https://doi.org/10.1198/016214502760047140.
Gräler, B., Pebesma, E., Heuvelink, G., 2016. Spatio-Temporal Interpolation using gstat. R J. 8, 204–218. https://doi.org/10.32614/RJ-2016-014.
Herold, M., Carter, S., Avitabile, V., Espejo, A.B., Jonckheere, I., Lucas, R., McRoberts, R. E., Næsset, E., Nightingale, J., Petersen, R., Reiche, J., Romijn, E., Rosenqvist, A., Rozendaal, D.M.A., Seifert, F.M., Sanz, M.J., De Sy, V., 2019. The Role and Need for Space-Based Forest Biomass-Related Measurements in Environmental Management and Policy. Surv. Geophys. 40, 757–778. https://doi.org/10.1007/s10712-019-09510-6.
Kyriakidis, P.C., 2004. A Geostatistical Framework for Area-to-Point Spatial Interpolation. Geogr. Anal. 36, 259–289. https://doi.org/10.1111/j.1538-4632.2004.tb01135.x.
Lohr, S.L., 2010. Sampling: Design and Analysis, second ed. Brooks/Cole, Boston.
McRoberts, R.E., Chen, Q., Domke, G.M., Ståhl, G., Saarela, S., Westfall, J.A., 2016. Hybrid estimators for mean aboveground carbon per unit area. For. Ecol. Manag. 378, 44–56. https://doi.org/10.1016/j.foreco.2016.07.007.
McRoberts, R.E., Liknes, G.C., Domke, G.M., 2014. Using a remote sensing-based, percent tree cover map to enhance forest inventory estimation. For. Ecol. Manag. 331, 12–18. https://doi.org/10.1016/j.foreco.2014.07.025.
McRoberts, R.E., Næsset, E., Gobakken, T., 2018. Comparing the stock-change and gain–loss approaches for estimating forest carbon emissions for the aboveground biomass pool. Can. J. For. Res. 48, 1535–1542. https://doi.org/10.1139/cjfr-2018-0295.
McRoberts, R.E., Næsset, E., Saatchi, S., Liknes, G.C., Walters, B.F., Chen, Q., 2019. Local validation of global biomass maps. Int. J. Appl. Earth Obs. Geoinformation 83, 101931. https://doi.org/10.1016/j.jag.2019.101931.
McRoberts, R.E., Næsset, E., Sannier, C., Stehman, S.V., Tomppo, E.O., 2020. Remote Sensing Support for the Gain-Loss Approach for Greenhouse Gas Inventories. Remote Sens. 12, 1891. https://doi.org/10.3390/rs12111891.
McRoberts, R.E., Wendt, D.G., Nelson, M.D., Hansen, M.H., 2002. Using a land cover classification based on satellite imagery to improve the precision of forest inventory area estimates. Remote Sens. Environ. 81, 36–44. https://doi.org/10.1016/S0034-4257(01)00330-3.
MINAGRI, MINAM, 2016. Marco Metodológico del Inventario Nacional Forestal y de Fauna Silvestre – Perú (No. Nº 253-2016-SERFOR-DE). Ministerio de Agricultura y Riego MINAGRI & Ministerio del Ambiente (MINAM), Lima.
MINAM, MIDAGRI, 2021. Nivel de referencia de emisiones forestales por deforestación bruta del Perú en el bioma Amazónico.
Næsset, E., McRoberts, R.E., Pekkarinen, A., Saatchi, S., Santoro, M., Trier, Ø.D., Zahabu, E., Gobakken, T., 2020. Use of local and global maps of forest canopy height and aboveground biomass to enhance local estimates of biomass in miombo woodlands in Tanzania. Int. J. Appl. Earth Obs. Geoinformation 93, 102138. https://doi.org/10.1016/j.jag.2020.102138.
Næsset, E., Ørka, H.O., Solberg, S., Bollandsås, O.M., Hansen, E.H., Mauya, E., Zahabu, E., Malimbwi, R., Chamuya, N., Olsson, H., Gobakken, T., 2016. Mapping and estimating forest area and aboveground biomass in miombo woodlands in Tanzania using data from airborne laser scanning, TanDEM-X, RapidEye, and global forest maps: A comparison of estimated precision. Remote Sens. Environ. 175, 282–300. https://doi.org/10.1016/j.rse.2016.01.006.
Nesha, M.K., Herold, M., De Sy, V., Duchelle, A.E., Martius, C., Branthomme, A., Garzuglia, M., Jonsson, O., Pekkarinen, A., 2021. An assessment of data sources, data quality and changes in national forest monitoring capacities in the Global Forest Resources Assessment 2005–2020. Environ. Res. Lett. 16, 054029 https://doi.org/10.1088/1748-9326/abd81b.
Ogle, S., Kurz, W., Green, C., Brandon, A., Baldock, J., Domke, G., Herold, M., Bernoux, M., Chirinda, N., Ligt, R., Federici, S., García-Apaza, E., Grassi, G., Gschwantner, T., Hirata, Y., Houghton, R., House, J., Ishizuka, S., Jonckheere, I., Waterworth, R., 2019. Chapter 2 Generic methodologies applicable to multiple land-use categories, in: 2019 Refinement to the 2006 IPCC Guidelines for National Greenhouse Gas Inventories. IPCC, p. 2.1-2.96.
Plataforma Geobosques, 2021. Mapas de Uso y Cambio de Uso Periodo 2013-2016.
Ploton, P., Mortier, F., Barbier, N., Cornu, G., Réjou-Méchain, M., Rossi, V., Alonso, A., Bastin, J.-F., Bayol, N., Bénédet, F., Bissiengou, P., Chuyong, G., Demarquez, B., Doucet, J.-L., Droissart, V., Kamdem, N.G., Kenfack, D., Memiaghe, H., Moses, L., Sonké, B., Texier, N., Thomas, D., Zebaze, D., Pélissier, R., Gourlet-Fleury, S., 2020. A map of African humid tropical forest aboveground biomass derived from management inventories. Sci. Data 7, 221. https://doi.org/10.1038/s41597-020-0561-0.
Réjou-Méchain, M., Barbier, N., Couteron, P., Ploton, P., Vincent, G., Herold, M., Mermoz, S., Saatchi, S., Chave, J., de Boissieu, F., Féret, J.-B., Takoudjou, S.M., Pélissier, R., 2019. Upscaling Forest Biomass from Field to Satellite Measurements: Sources of Errors and Ways to Reduce Them. Surv. Geophys. 40, 881–911. https://doi.org/10.1007/s10712-019-09532-0.
Réjou-Méchain, M., Muller-Landau, H.C., Detto, M., Thomas, S.C., Le Toan, T., Saatchi, S. S., Barreto-Silva, J.S., Bourg, N.A., Bunyavejchewin, S., Butt, N., Brockelman, W.Y.,

Cao, M., Cárdenas, D., Chiang, J.-M., Chuyong, G.B., Clay, K., Condit, R., Dattaraja, H.S., Davies, S.J., Duque, A., Esufali, S., Ewango, C., Fernando, R.H.S., Fletcher, C.D., Gunatilleke, I.A.U.N., Hao, Z., Harms, K.E., Hart, T.B., Hérault, B., Howe, R.W., Hubbell, S.P., Johnson, D.J., Kenfack, D., Larson, A.J., Lin, L., Lin, Y., Lutz, J.A., Makana, J.-R., Malhi, Y., Marthews, T.R., McEwan, R.W., McMahon, S.M., McShea, W.J., Muscarella, R., Nathalang, A., Noor, N.S.M., Nytch, C.J., Oliveira, A. A., Phillips, R.P., Pongpattananurak, N., Punchi-Manage, R., Salim, R., Schurman, J., Sukumar, R., Suresh, H.S., Suwanvecho, U., Thomas, D.W., Thompson, J., Uríarte, M., Valencia, R., Vicentini, A., Wolf, A.T., Yap, S., Yuan, Z., Zartman, C.E., Zimmerman, J.K., Chave, J., 2014. Local spatial structure of forest biomass and its consequences for remote sensing of carbon stocks. Biogeosciences 11, 6827–6840. https://doi.org/10.5194/bg-11-6827-2014.

Réjou-Méchain, M., Tanguy, A., Piponiot, C., Chave, J., Hérault, B., 2017. BIOMASS: an R package for estimating above-ground biomass and its uncertainty in tropical forests. Methods Ecol. Evol. 8, 1163–1167. https://doi.org/10.1111/2041-210X.12753.

Rodríguez-Veiga, P., Wheeler, J., Louis, V., Tansey, K., Balzter, H., 2017. Quantifying Forest Biomass Carbon Stocks From Space. Curr. For. Rep. 3, 1–18. https://doi.org/10.1007/s40725-017-0052-5.

Romijn, E., Lantican, C.B., Herold, M., Lindquist, E., Ochieng, R., Wijaya, A., Murdiyarso, D., Verchot, L., 2015. Assessing change in national forest monitoring capacities of 99 tropical countries. For. Ecol. Manag. 352, 109–123. https://doi.org/10.1016/j.foreco.2015.06.003.

Saatchi, S., Marlier, M., Chazdon, R.L., Clark, D.B., Russell, A.E., 2011. Impact of spatial variability of tropical forest structure on radar estimation of aboveground biomass. Remote Sens. Environ., DESDynI VEG-3D Special Issue 115, 2836–2849. https://doi.org/10.1016/j.rse.2010.07.015.

Santoro, M., Cartus, O., 2021. ESA Biomass Climate Change Initiative (Biomass_cci): Global datasets of forest above-ground biomass for the years 2010, 2017 and 2018, v3. Doi: https://doi.org/10.5285/5F331C418E9F4935B8EB1B836F8A91B8.

Särndal, C.-E., Swensson, B., Wretman, J., 1992. Model assisted survey sampling. Springer Science & Business Media.

SERFOR, 2020. Inventario nacional forestal y de fauna silvestre: Informe de resultados del panel 1. Lima.

Ståhl, G., Heikkinen, J., Petersson, H., Repola, J., Holm, S., 2014. Sample-Based Estimation of Greenhouse Gas Emissions From Forests—A New Approach to Account for Both Sampling and Model Errors. For. Sci. 60, 3–13. https://doi.org/10.5849/forsci.13-005.

Ståhl, G., Saarela, S., Schnell, S., Holm, S., Breidenbach, J., Healey, S.P., Patterson, P.L., Magnussen, S., Næsset, E., McRoberts, R.E., Gregoire, T.G., 2016. Use of models in large-area forest surveys: comparing model-assisted, model-based and hybrid estimation. For. Ecosyst. 3, 5. https://doi.org/10.1186/s40663-016-0064-9.

Zeileis, Achim, Hothorn, Torsten, 2002. Diagnostic Checking in Regression Relationships. R News 2 (3), 7–10. https://cran.r-project.org/doc/Rnews/Rnews_2002-3.pdf, 2002.